Section A-Research paper
ISSN 2063-5346

CFD study of counter-current flow behavior and liquid holdup in random packed column

Abdulwahid A.A.S Al-Haddad[1*], Eflita Yohana[1] , Tony Suryo Utomo[1] , Asim Aamir[1],and Zafran Ullah[2]
[1]Department of Mechanical Engineering, Diponegoro University, Jl. Prof. Sudharto, SH, Semarang 50275, Indonesia
[2]Department of Chemical Engineering, Diponegoro University, Jl. Prof. Sudharto, SH, Semarang 50275, Indonesia
Corresponding Author*:abdulwahid.alhaddad@yahoo.com
DOI:10.48047/ecb/2023.12.si4.1563

Abstract

In this study, countercurrent gas-liquid flow simulations using computational fluid dynamics (CFD) were conducted for random packings of Raschig rings. The random packing structure was constructed using gravity simulation, and the meshing quality was improved using a volume expansion-recovery method. In this study, the contacting issue between the gas and liquid phases was investigated using the volume of fluid model. Also CFD gas–liquid interface area of the small-scale absorbers is validated by the experimental data. The effect of rasching ring distribution in the packed column visualized by cross section plane contour of the gas velocity. The gas velocity is limited at 0.011 m/s in most regions. A high gas velocity can be observed in the regions with the absence of rasching rings. The maximum velocity reaches 0.1 m/s, and these regions are mostly located in the near-wall region for all four cases .The liquid holdup estimated from the simulation and compared with the available correlation ,and the results reveal that the estimated CFD liquid holdup h_L is in good agreement with existing correlations experimental data.

Keywords: Random packed column, Liquid holdup, Countercurrent flow, Multiphase, CFD simulation

Nomenclature

A_i	gas liquid interface area	θ_w	Contact angle [°]
a_i	Interfacial area concentration [m^2 /m^3]	K	Curvature of local surface/interface[1/m]
a_p	Specific area [m^2 /m^3]	μ_g	Viscosity of gas [Pa·s]
C_{CO_2}	CO_2 concentration [ppmv]	μ_L	Viscosity of liquid [Pa·s]
F_σ	Surface tension force [N]	ρ_g	Density of gas [kg/m^3]
P	Pressure [Pa]	ρ_L	Density of liquid [kg/m^3]
u_G	Gas velocity	Subscripts	
u_L	Liquid velocity	e	Effective
V_L	Liquid volume [m3]	G	gas
V_C	Empty column volume [m3]	L	Liquid
Z	Column height [m]	i	interface
Greek symbols			
α	Volume fraction of liquid [-]	VOF	Volume Of fluid
$\in$	Packing Porosity [-]		

1.Introduction

Packings are commonly employed in columns for distillation, absorption, and stripping. Effective mass transfer in packing decreases a column's height and decreases construction cost. Alternatively, improved packing can increase the number of transfer units, reducing reflux in a distillation column and absorption solvent consumption, resulting in lower operating costs and higher productivity in revamping[1]. Carbon dioxide (CO_2) emissions from the combustion of fossil are thought to be a major cause to climate change [2]. One of the realistic ways to minimize CO_2 emissions is to capture CO_2 from big point sources, transport it to a storage location, and geologically deposit it there[3]. Because of various available technologies, post-combustion capture is a common configuration in CO_2 capture, and existing fossil fuel power plants may be modified to add CO_2 capture equipment[4]. Packed columns are often employed in the post-combustion process to collect CO_2 by increasing the contact area between the gas and liquid phases. To enhance packed column performance and CO_2 capture efficiency, it is crucial to examine mass transfer area and liquid holdup behavior. Several experimental and CFD studies have been conducted to investigate the hydrodynamics of countercurrent flow in packed columns. Zhang et al.[5] Examined experimentally The ability of a counter-flow packing tower to transmit heat and mass (number of mass transfer units NTUm), as well as its impact on system performance. Tan et al.[6] Investigated the heat and mass transfer characteristics of the moist air–water counter-current flow for large-scale air separation units in a randomly packed air cooling tower (RPACT). They developed a computational fluid dynamics model for 3D porous media (CFD) alongside mass transfer equations. Liu et al[7]. Proposed a numerical method for modeling the distillation process in a randomly packed column. Without using the calculated turbulent mass transfer diffusivity or the empirical turbulent Schmidt number, the proposed model can predict the axial and radial concentration distributions along the column. Trubyanov et al.[8] Examined the effects of temperature, pressure, and loading on the pressure drop, flooded vapor flow rate, partition coefficient, separation factor, HETP, velocity, and mass transfer coefficient in small-scale randomly packed columns for high-pressure distillation. Fu et al.[9] developed a framework for studying the liquid–gas countercurrent flow hydrodynamics in a random packed column with pall rings. To analyze the entrance effect and the wall influence in the packed column, the radial pall ring distribution, velocity, and liquid holdup profiles are collected in addition to the column-averaged information .Kang et al.[1]Proposed an innovative method for simulating the hydrodynamics of countercurrent gas–liquid flow in random packing .Haroun et al.[10]Used Volume Of Fluid (VOF) model to anticipate the gas and liquid contact area of a Mellapak 250X REU with countercurrent flows having one velocity inlet and one pressure outlet boundary. Kang et al.[11]Investigated the flow field of random packing using Volume Of Fluid (VOF) model in CFD software .Yu et al.[12] Investigated numerically and experimentally the heat and mass transfer performance of a counter-flow spray concentration tower under diverse operating conditions.

2.Methodology

2.1. Mathematical formulations

For the 3D multiphase flow analysis in a typical model of a random packed column, the commercial CFD software ANSYS Fluent 2020 R2 was used. The numerical model involves solving the mass and momentum conservation equations. Multiphase fluid separation is modeled by fluid (VOF) method.

The mass conservation equation expressed as:

$$\frac{\partial \rho}{\partial t} + \nabla.(\rho u) = 0 \quad (1)$$

And the momentum equation expressed as:

$$\frac{\partial \rho u}{\partial t} + \nabla.(\rho u u) = -P + \mu \nabla^2 u + \rho g + F_\sigma \quad (2)$$

Where ρ is the density,μ is the viscosity, P is the pressure, and F_σ is the surface tension force at the liquid-gas interface.

Density and viscosity are averaged by the liquid and gas phase volume fraction as :

$$\rho = \rho_L \alpha + \rho_g (1 - \alpha) \quad (3)$$

$$\mu = \mu_L \alpha + \mu_g (1 - \alpha) \quad (4)$$

Where α is the volume fraction of liquid phase.

The interfacial surface tension force F_σ is computed as:

$$F_\sigma = \sigma k \nabla \alpha \, , k = -\nabla . \frac{\nabla \alpha}{|\nabla \alpha|} \quad (5)$$

Where σ is the surface tension coefficient, and k is the local mean curvature.

On the wall region , the term $\frac{\nabla \alpha}{|\nabla \alpha|}$ expressed as :

$$\frac{\nabla \alpha}{|\nabla \alpha|} = n_w cos\theta_w + t_w sin\theta_w \quad (6)$$

Where n_w,and t_w are the unit normal and tangential vectors respectively. And θ_w is the contact angle between the gas and liquid interface, the contact angle is set as 70° for the liquid and gas with plastic rasching ring walls[13]. The transport of the volume fraction a is governed by:

$$\frac{\partial \alpha}{\partial t} + \nabla . (u\alpha) = 0 \quad (7)$$

The volume fraction α can be computed in each computing cell using the VOF method. Then, an iso-surface that corresponds to α= 0.5 is created in order to recreate the gas-liquid interface[14]. The CFD computed a_i is expressed as :

$$a_i = \frac{A_i}{V_c} \quad (8)$$

Where , A_i , represents the gas liquid interface area , V_c is the volume of the empty column .

2.2. Random packing generation

The process of generating the random packing was done by employing gravity, which is a motion study in SOLIDWORKS®. A column as a small absorber with 25mm diameter and 100 mm height created. At the top of the absorber, a track was built. The track filled with more than 90 cylinder with 6 mm diameter and 6 mm in height which is will be replaced latterly with the rasching rings element that has outer diameter of 6 mm, inner diameter 4 mm and 6 mm of height. Using the cylinder instead of the rasching ring directly in the simulation due to avoid the large contacting between the rasching ring walls during the motion study. Figure 1, shows the atomic stacking technique

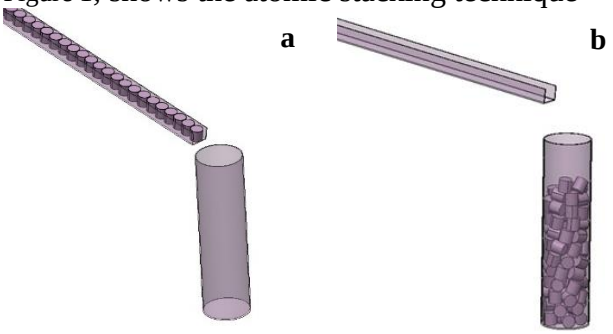

Figure 1. stacking technique (a)before stacking, (b) after stacking

The packing cylinder set as unfixed elements while the column , and the path set as fixed , the settings of the motion is shown in **Error! Reference source not found.**.

The randomly packing is generated by the collision between packings .When the simulation started, the packing cylinders fell into the column by gravity and formed a stack as shows in Figure 1(b). After the packing done then the cylinder replaced with the rasching ring packing elements to create the final random column, but there still problem after replacing the elements and export the geometry to make the mesh. There is dead zone appears between the packing elements due to the contact area during the stacking motion, which prevent Ansys from generating the mesh. To overcome this problem the diameter and height of the packing cylinder elements expanded to 6.3 mm and the inner diameter of the column reduced to 25.1 mm. after the stacking process is done the sizes is returned to the original (expansion and recovery method). The height of random packing structured was more than 80

mm, the cylinders stacking elements replaced by the original packing elements "rasching rings ". for reduce the computational cost the packed column cut with height of 22mm to create the flow field. The flow field of 25.4 mm and 22 in height was filled with 31.8 rasching ring elements. Figure 2 shows the flow field after the replacement and caping the absorber from the top and the bottom. 4 holes at the top, and 4 holes at the bottom were created will be used in the ANSYS Workbench to create the fluid domain. The wholes have the diameter of 5 mm and centered with r = 6mm from the center.

Table 1. Setting of the motion study in **SOLIDWORKS®**

Frame number (per second)	16
Geometry accuracy	10(maximum value)
3D contact resolution	10(maximum value) to prevent the interpenetration of packings
Gravity (m/s^2)	9.8
Packings	Floating and contactable
Column and track	Fixed and contactable

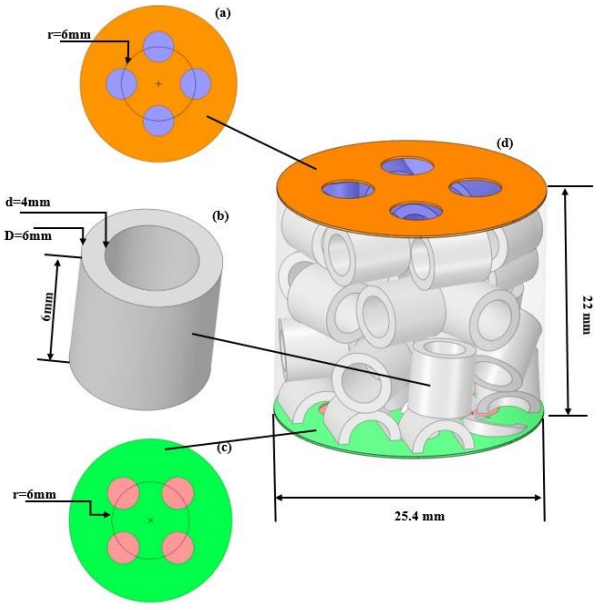

Figure 2.(a) The arrangement of 4 liquid drip holes at the top surface of the packed column; (b) Design and dimension details of the rasching ring in the packed column; (c)The arrangement of 4 gas holes at the bottom surface of the packed column;(d) Schematic of the flow domain showing the arrangement of the rasching rings inside the packed column.

Column-averaged porosity ∈ and specific area a_p are two significant geometrical characteristics in the random packed column that are directly connected to packed column performance. The Packing characteristics were calculated as flow :

Specific area :

$$a_p = \frac{Surface\ area\ of\ the\ packed\ material}{Volume\ of\ the\ column} = 627.69\ \frac{m^2}{m^3}$$

Porosity:

$$\in = \frac{the\ void\ region}{Volume\ of\ the\ packed\ column} = 0.7336$$

2.3.Problem setup and boundary conditions

The created geometry in **SOLIDWORKS®** imported into DesignModeler to prepare the fluid domain for mesh generation. The raschinng rings subtracted from the fluid domain. Figure 3, shows the fluid domain. The fluid domain transferred to Fluent (with Fluent mesh) to create the mesh . The computational domain is discretized into polyhedral mesh elements. A snapshot of the generated mesh is shown in Figure 4. A total of 103796 mesh cells is generated with maximum surface mesh skewness of 0.78, and minimum orthogonal quality of 0.20.

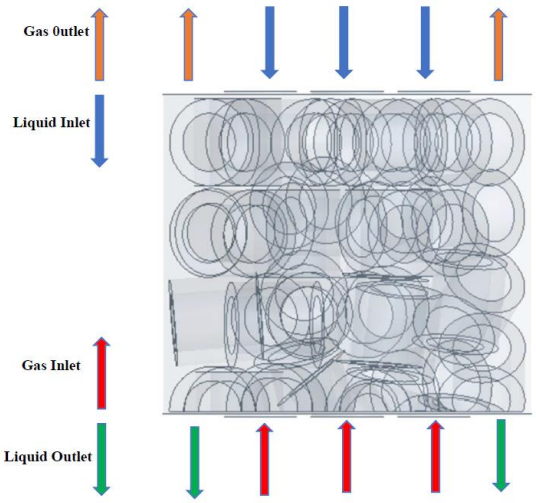

Figure 3. The fluid domain

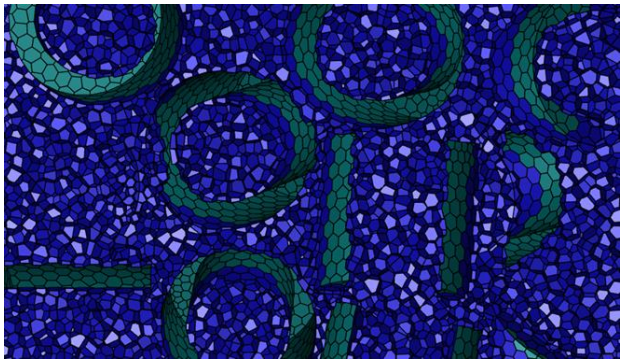

Figure 4. snapshot of the CFD mesh generated in the computational domain.

A three-dimensional single precision, serial processing ANSYS Solver is opened. Pressure-based type solver runs a transient fluid flow process. The numerical approach is based on an unsteady Eulerian Volume Of Fluid (VOF) two-phase. The primary phase set as Air and the secondary phase is water liquid, the surface tension coefficient set a constant value of 0.0728 N/m.Also the wall adhesion included to set the contact angle of the liquid-gas interface contact angle with the packing wall. The boundary operating conditions are shown in **Error! Reference source not found.**. The momentum equations is spatially discretized using the second-order upwind method and the volume fraction is compressive. and the time term is discretized by implicit scheme. The pressure–velocity coupling equation is derived using the coupled algorithm. The solution method for pressure is the "PRESTO!" equation. The turbulent kinetic energy, and specific dissipation rate are all discretized by the first-order upwind method. Additional details are shown in *Table 3*.

Table 2. boundary condition of the random packed column

Position	Boundary type	Material	Detail parameters and values
Top Liquid inlet	Velocity inlet	Water	Liquid velocity (0.1-0.5)$\frac{m}{s}$; liquid volume fraction =1
Gas outlet	Pressure outlet	Air	Gauge pressure = 0
Bottom Gas inlet	Velocity inlet	Air	Gas velocity constant = 0.1 m/s
Liquid outlet	Pressure outlet	water	Gauge pressure = 0
Column wall	Wall		Stationary wall, no slip
Rasching rings wall	Wall	Plastic	Stationary wall, no slip, wall adhesion contact angle 70°

Table 3. Solution parameter settings.

Parameter	Details
Volume fraction	Implicit

parameter	
Viscous model	SST K-ω
Packing type	Plastic Rasching Ring
Number of time step	1000
Maximum number of iterations	20
Time step	0.001 s
Convergence of residual deviation	0.001
Gravity	Direction: -Y, 9.81 m/s^2

3. Results and discussion

3.1. Stationary State Determination

The criteria used to determine the system reached steady state is the air volume fraction. **Error! Reference source not found.**. shows the average volume fraction of the fluid domain with different liquid velocity inlet. The figure illustrates that independent of changes in liquid velocity or flow rate, the flow field requires 0.45 seconds to achieve steady state. The average air volume fraction would certainly drop as liquid velocity increased.

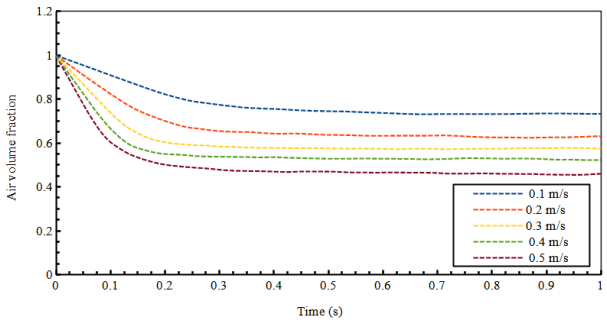

Figure 5. average volume fraction with different inlet liquid flow rate

3.2. Mesh Independent Study

A mesh independence study was performed to improve the amount of mesh elements employed in the simulations in order to balance the accuracy and efficiency of the CFD model. The countercurrent flow simulations were conducted at a constant liquid velocity inlet of 0.5 m/s. The transient average air volume fraction curves are plotted in **Error! Reference source not found.** for four different number of mesh elements. The four different mesh were 103.8 $\times 10^3$, 144.7 $\times 10^3$, 294.3 $\times 10^3$, 534.8 $\times 10^3$ cells .The figure shous that for 534.8$\times 10^3$,and 294.3$\times 10^3$ reaches the steady state after 0.6 s . With mesh of 144.7 $\times 10^3$,and 103.8 $\times 10^3$ the system reaches the steady state after 0.4 s , with slight difference in the average air volume fraction. And the gas liquid interface area compression shown in Table 4 for the four different mesh the table shows that there is a little difference between the gas-liquid interface area .The 103.8 $\times 10^3$ mesh element resolution is selected for the following countercurrent flow simulations due to the available computer capability.

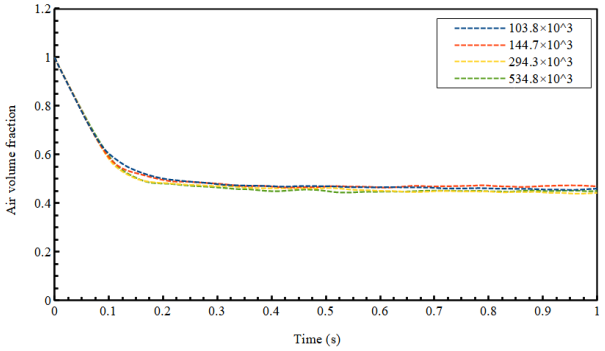

Figure 6. Averaged Air volume fraction with different mesh size resolution. The simulations are run at a constant liquid velocity of 0.5 m/s

3.3. Mass transfer area

The gas-liquid interface area collected in simulations is compared with the available correlations derived experiments to validate the accuracy of the CFD model. It is difficult to determine interface area concentration a_i directly in experiments. Rather than measuring

a_i, the effective mass transfer area a_e can be determined using the CO_2 absorption rate and the measured mass transfer coefficient K_g' as shown below:

$$a_e = \frac{u_g}{K_G' ZRT} \ln\left(\frac{C_{CO_{2,in}}}{C_{CO_{2,out}}}\right) \quad (9)$$

Where, Z is the packed column height, R is the gas constant, and T is the temperature. $C_{CO_{2,in}}$,and $C_{CO_{2,out}}$ are the averaged CO_2 concentrations at the inlet and outlet of the packed column, respectively. More details of calculating a_e can be found in the literature [15], [16]. Because the reaction usually takes place at the liquid-gas interface, the liquid-gas interfacial area should be comparable to the effective mass transfer area predicted by Eq.(9). The gas–liquid interface area calculated by using the iso-surface curve in Ansys Fluent®, where the liquid and gas phase volume fraction set were at 0.5 as shown in **Error! Reference source not found.**. The estimated a_i from CFD is then compared to the correlation proposed by Onda et al.[17]. The effective transfer area a_e for the correlation is given as:

$$\frac{a_e}{a_p} = 1 - \exp\left\{-1.45\left(\frac{\sigma_c}{\sigma}\right)^{0.75}\left(\frac{L}{a_p \mu_L}\right)^{0.1}\left(\frac{L^2 a_p}{\rho_L^2 g}\right)^{-0.05}\left(\frac{L^2}{\rho_L \sigma a_p}\right)^{0.2}\right\} \quad (10)$$

Where , a_p is specific area,σ_c is the critical surface tension of packing material , σ is the surface tension , L is the superficial mass velocity of the liquid ,μ_L is the liquid viscosity , ρ_L is the liquid density , g is the gravitational constant .

The comparison between the CFD-computed a_i and the correlation is shown in Figure 13 . The area in **Error! Reference source not found.**. Is all normalized by the total column specific area a_p.

Table 4. gas-liquid interface area with different mesh size resolution

Number of Elements	Skewness & Minimum Orthogonal Quality	G-L Interface Area
103.8 ×10³	0.78 & 0.20	0.003731648
144.7 ×10³	0.73 & 0.20	0.0037982762
294.3 ×10³	0.79 & 0.20	0.0035830068
534.8 ×10³	0.74 & 0.20	0.0034059682

As we can see in **Error! Reference source not found.**, The simulated interfacial area increases with the increase of the liquid velocity which is similar to the correlations . The confidence interval of 20% is added for the simulated interfacial area and the correlation of Onda et al.[17] as reference. Overall, the CFD liquid–gas interfacial area is close to the effective mass transfer area predicted by Eq. (10).

3.4. Effect of rasching ring on the gas velocity

The gas velocity magnitude distribution at the center cross section plane is shown in **Error! Reference source not found.** ,Figure 10 , Figure 11 ,and Figure 12 with liquid velocity u_L = 0.2, 0.3 . 0.4 ,0.5 m/s respectively. As shown in the contours , the gas velocity is limited at 0.011 m/s in most regions. A high gas velocity can be observed in the regions with the absence of rasching rings. The maximum velocity reaches 0.1 m/s, and these regions are mostly located in the near-wall region for all four cases.

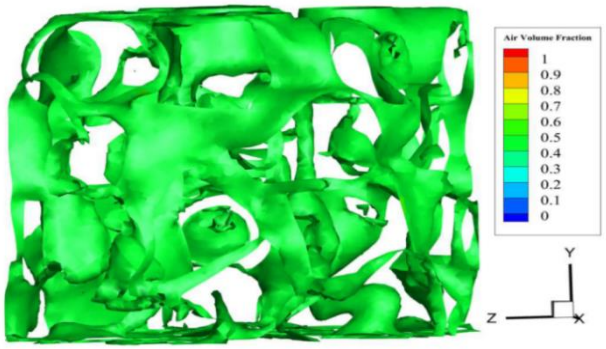

Figure 7. Iso-surface of air volume fraction at α = 0.5

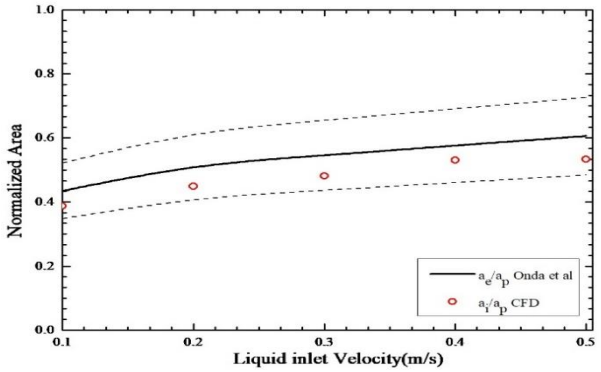

Figure 8. Comparison of the CFD-predicted interfacial area with the empirical mass transfer area given by the correlation

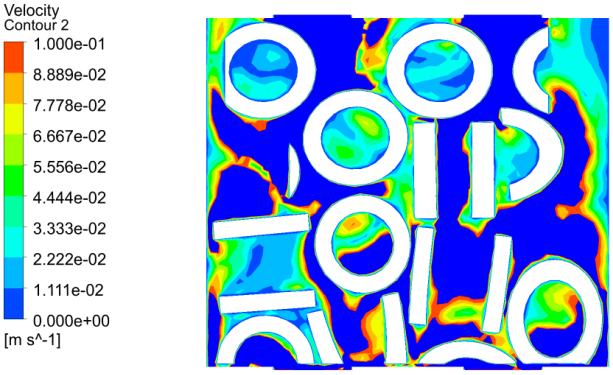

Figure 9. Gas velocity magnitude on the center cross section of the packed column at liquid velocity of 0.2 m/s

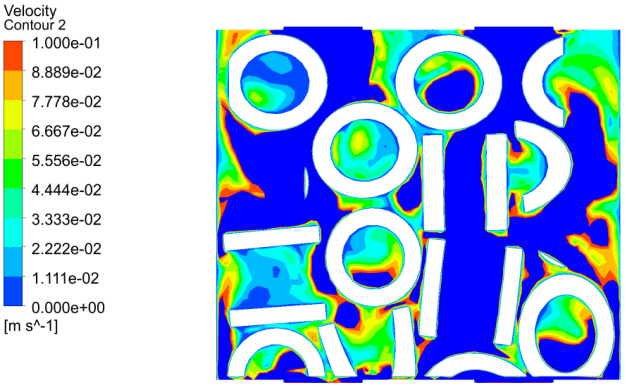

Figure 10. Gas velocity magnitude on the center cross section of the packed column at liquid velocity of 0.3 m/s

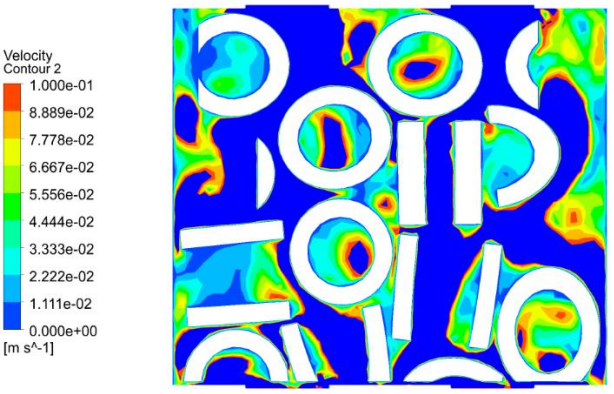

Figure 11. Gas velocity magnitude on the center cross section of the packed column at liquid velocity of 0.4 m/s

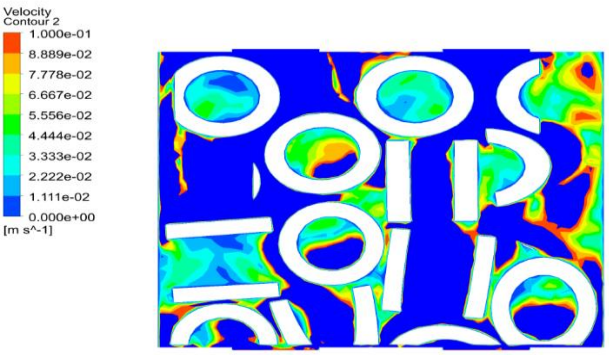

Figure 12. Gas velocity magnitude on the center cross section of the packed column at liquid velocity of 0.4 m/s

3.5. The Influence of Liquid Flow Rate on Liquid Hold Up

In a packed column, the liquid holdup refers to the fraction or percentage of the column volume occupied by liquid. It is an important parameter in the design and optimization of packed column processes, as it affects the mass transfer and separation efficiency of the column .The liquid holdup can be predicted from the simulation by the fraction of liquid volume (V_L) over the total empty column volume (V_C) . ***Error! Reference source not found.*** shows a comparison of liquid holdup between CFD result and the available correlations data. The compared correlation is Stichlmair, et al.[18].The correlation of the liquid holdup is expressed as ;

$$h_L = 0.555\left(u_L^2 \frac{a_p}{g \in^{4.65}}\right)^{1/3} \quad (11)$$

Where h_L is the liquid holdup , and $u_L$is the liquid velocity . As shown in Figure 13 .The

liquid holdup increase by increasing the liquid velocity ,and the simulation result is close the correlation of stichlmair et al. the correlation is wildly used on random packing.

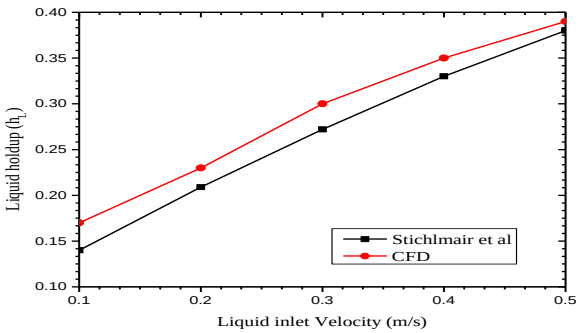

Figure 13. A comparison of liquid hold up among simulation result and the available correlation .

4. Conclusion

The VOF model in is used in this work to study the flow field of counter current flow in random packing. The model validated with the available correlation using the gas-liquid interface area and the results were in a good agreement with the correlation,and it was observed that gas-liquid interface area increase as the liquid velocity increase . and the effect of the rasching rings wall observed through visualization of contour for four different liquid velocities . The maximum velocity reaches 0.1 m/s, and these regions are mostly located in the near-wall region for all four cases. And the liquid holdup estimated and compared with the available correlation and its seemed close to the correlation ,the values of the liquid holdup increasing with the increase of liquid velocity.

References

[1] J.-L. Kang, Y.-C. Ciou, D.-Y. Lin, D. S.-H. Wong, and S.-S. Jangb, "Investigation of hydrodynamic behavior in randompacking using CFD simulation.pdf," *Chem. Eng. Res. Des.*, vol. 147, pp. 43–54, 2019, [Online]. Available: https://doi.org/10.1016/j.cherd.2019.04.037

[2] L. M. Bert Metz , Ogunlade Davidson . Heleen de Coninck , Manuela Loos, "IPCC Special Report on Carbon Dioxide Capture and Storage," *Advances in Chemical Engineering*, vol. 58. 2005. doi: 10.1016/bs.ache.2021.10.005.

[3] R. S. Haszeldine, "Carbon Capture and Storage: How Green Can Black Be?," *Science*, vol. 325. pp. 1647–1652, 2009. [Online]. Available: http://www.ccsassociation.org/why-ccs/ccs-projects/current-projects/

[4] and J. R. L. Kenji Sumida, David L. Rogow, Jarad A. Mason, Thomas M. McDonald, Eric D. Bloch, Zoey R. Herm, Tae-Hyun Bae, "Carbon Dioxide Capture in Metal?Organic Frameworks." Chem. Rev, pp. 724–781, 2011.

[5] L. Zhang, X. Liu, H. Wei, and X. Zhang, "Experimental study and analysis of heat and mass transfer ability of counter-flow packing tower and liquid desiccant dehumidification system," *Energy and Buildings*, vol. 158. pp. 150–161, 2018. doi: 10.1016/j.enbuild.2017.10.016.

[6] H. Tan, N. Wen, and Z. Ding, "Numerical study on heat and mass transfer characteristics in a randomly packed air cooling tower for large-scale air separation systems," *Int. J. Heat Mass Transf.*, vol. 178, p. 121556, 2021, doi: 10.1016/j.ijheatmasstransfer.2021.121556.

[7] G. B. Liu, K. T. Yu, X. G. Yuan, and C. J. Liu, "A numerical method for predicting the performance of a randomly packed distillation column," *International Journal of Heat and Mass Transfer*, vol. 52, no. 23–24. pp. 5330–5338, 2009. doi: 10.1016/j.ijheatmasstransfer.2009.06.038.

[8] M. M. Trubyanov, G. M. Mochalov, V. M. Vorotyntsev, and S. S. Suvorov, "High pressure distillation Simultaneous impact of pressure , temperature and loading on separation performance during distillation of high purity gases in high performance randomly-packed columns.pdf," *Sep. Purif. Technol.*, vol. 135, pp. 117–126, 2014, doi: 10.1016/j.seppur.2014.08.010.

[9] Y. Fu, J. Bao, R. Singh, C. Wang, and Z. Xu, "Investigation of countercurrent flow profile and liquid holdup in random.pdf," *Chem. Eng. Sci. J.*, vol. 221, pp. 115693–115704, 2020, [Online]. Available: https://doi.org/10.1016/j.ces.2020.115693

[10] Y. Haroun, L. Raynal, and P. Alix, "Prediction of effective area and liquid hold-up in structured packings by CFD," *Chem. Eng. Res. Des.*, vol. 92, pp. 2247–2254, 2014, [Online]. Available: http://dx.doi.org/10.1016/j.cherd.2013.12.029

[11] J.-L. Kang, W.-F. Chen, D. S.-H. Wong, and S.-S. Jang, "Evaluation of Gas-Liquid Contact Area and Liquid Holdup of Random packing using CFD simulation," in *6th International Symposium on Advanced Control of Industrial Processes (AdCONIP)*, 2017. doi: 978-1-5090-4396-5/17/$31.00 ©2017 IEEE.

[12] J. Yu, S. Jin, and Y. Xia, "Experimental and CFD investigation of the counter-flow spray concentration tower in solar energy air evaporating separation saline wastewater treatment system," *Int. J. Heat Mass Transf.*, vol. 144, p. 118621, 2019, doi: 10.1016/j.ijheatmasstransfer.2019.118621.

[13] H. Z. Ying Ma , Xinyu Cao , Xinjian Feng , Yongmei Ma, "Fabrication of super-hydrophobic film from PMMA with intrinsic water contact angle below 90_," *Polymer (Guildf).*, vol. 48, pp. 7455–7460, 2007.

[14] H.-J. B. Adel Ataki, "Experimental and CFD Simulation Study for the Wetting of a Structured Packing Element with Liquids*," *Chem. Eng. Technol*, vol. 29, no. 3, 2006, doi: 10.1002/ceat.200500302.

[15] R. Tsai, "Mass Transfer Area of Structured Packing," The University of Texas at Austin, 2010.

[16] C. Wang, "Mass Transfer Coefficients and Effective Area of Packing," The University of Texas at Austin, 2015.

[17] and Y. O. K. Onda, H. Takeuchi, "Mass transfer coefficients between gas and liquid phases in packed columns." Journal of chemical engineering of Japan, vol. 1, pp. 56-62, 1968. doi: 10.1252/jcej.1.56.

[18] J. L. B. and J. R. F. J. Stichlmair, "General model for prediction of pressure drop and capacity of countercurrent gas/liquid packed columns." Gas Separation 8 Purification, pp. 19–28, 1989.